Available online at www.sciencedirect.com
ScienceDirect
Trans. Nonferrous Met. Soc. China 28(2018) 1521−1529
Transactions of Nonferrous Metals Society of China
www.tnmsc.cn

Precipitation location of secondary phase and microstructural evolution during static recrystallization of as-cast Ti−25V−15Cr−0.3Si titanium alloy

Yan-chun ZHU[1], Qing-xue HUANG[1,2], Xiao-hui SHI[2], Mei-rong SHUAI[1], Wei-dong ZENG[3], Yong-qing ZHAO[4], Zhi-quan HUANG[1], Li-feng MA[1]

1. Collaborative Innovation Center of Taiyuan Heavy Machinery Equipment, Taiyuan University of Science and Technology, Taiyuan 030024, China;
2. School of Materials Science and Engineering, Taiyuan University of Technology, Taiyuan 030024, China;
3. State Key Laboratory of Solidification Processing, Northwestern Polytechnical University, Xi'an 710072, China;
4. Northwest Institute for Nonferrous Metals Research, Xi'an 710076, China

Received 24 April 2017; accepted 10 December 2017

Abstract: The microstructural evolution and precipitation location of the secondary phase of an as-cast Ti−25V−15Cr−0.3Si titanium alloy were investigated via isothermal compression experiments and heat treatment. The average aspect (length-to-width) ratio, average area and size of the grains at different heat treatment temperatures and holding time were analyzed and the effects of deformation and annealing time on the grain area and size were considered. It was found that the grain size was strongly influenced by the height reduction and holding time. Grain growth was significant when annealing time increased from 10 min to 2 h at 950 °C and height reduction of 30%; however, grain growth was minimal at annealing time between 2 and 4 h. Many dispersion particles were observed to form in continuous chains; the precipitation location was confirmed to be along initial grain boundaries, and the dispersion particles were identified to be Ti_5Si_3 phase by TEM.

Key words: Ti−25V−15Cr−0.3Si titanium alloy; static recrystallization; microstructural evolution; grain size; secondary phase; precipitation location

1 Introduction

Ti−V−Cr-series burn-resistant titanium alloys have attracted increasing attention because of their ability to avoid "titanium fire" and, in 1996, the Northwest Institute for Nonferrous Metal Research of China developed the alloy Ti−25V−15Cr−0.3Si as a new Ti−V−Cr burn-resistant titanium alloy [1]. However, it is difficult to obtain a fine β-grain microstructure through hot deformation in Ti−25V−15Cr−0.3Si, possibly due to the pile-up of dislocation near the alloying element, which is present in high levels (up to 40%). To develop Ti−25V−15Cr−0.3Si alloy with fine β-grain microstructures, it is necessary to study the static recrystallization (SRX) behavior and the effect of heat treatment parameters on microstructure evolution.

IVASISHIN et al [2] studied the precipitation and recrystallization behavior during continuous heat treatment of three β Ti alloys with different molybdenum equivalents (VT22, Ti-15-3 and TIMETAL-LCB). They found that precipitation velocity of the omega and alpha phases in the highly-alloyed materials (TIMETAL-LCB and Ti-15-3) was slower than that in VT22. SEMIATIN et al [3−8] studied SRX of Ti–6Al–4V and developed a model to predict properties of that alloy after deformation and annealing at different temperatures. ZHEREBTSOV et al [9] studied the spheroidization behavior of a colony microstructure in a Ti−6Al−4V alloy during warm working and subsequent annealing at 600 and 800 °C. XU et al [10] examined the effects of hot deformation on the microstructure of β-C titanium

Foundation item: Projects (51501122, 51604181) supported by the National Natural Science Foundation of China; Project (20172009) supported by the Postdoctoral Sustentation Fund of Taiyuan University of Science and Technology, China; Project (20132016) supported by the Research Fund for the Doctoral Program of Higher Education of China; Project (201501004-8) supported by the Jincheng Science and Technology Plan Project, China; Project (U1510131) supported by NSFC-Shanxi Coal-based Low-carbon United Fund and "Shanxi Young Scholars" Program, China; Project (201603D121010) supported by Key R&D Program of Shanxi Province, China
Corresponding author: Qing-xue HUANG; Tel: +86-351-6010200; E-mail: hqx6688@126.com
DOI: 10.1016/S1003-6326(18)64793-4

alloy during heat treatment, and deemed that the deformed specimens heat-treated at 800 °C for 70 min and then air-cooled consist of fine grains which may improve mechanical properties of this alloy. LI et al [11] analyzed the effects of heat treatment parameters on the microstructure of Ti−5Al−2Sn−2Zr−4Mo−4Cr alloy, and pointed out that the volume fraction of primary α phase decreased and the amount and width of the secondary α phase increased with the increase of heating temperature. Recently, FANG et al [12] have studied the effect of cyclic heat treatment on microstructures of as-cast Ti−46Al−6Nb alloy, and found that the extending holding time and increasing the cyclic times of heat treatment can effectively eliminate the β-segregation at the grain boundary and the interlamellar position. SONG et al [13] investigated the precipitation of ω_o phase in annealed TiAl alloys containing high Nb, and pointed out that the average size and volume fraction of ω_o phase increased accordingly with the increase of Nb addition. Thus, it is effective to research the precipitation location of the secondary phase by means of heat treatment.

In general, deformed β grains can be recrystallized by performing an additional heat treatment, to produce a finer microstructure in β Ti alloys. Performing an additional heat treatment may also produce a recovered microstructure in which precipitates may be more uniform than that in the deformed condition [14]. It is necessary to study SRX behavior of the Ti−25V−15Cr−0.3Si alloy to understand the effects of deformation and heat treatment parameters on microstructural evolution. Isothermal compression and heat treatment tests were used to study the effects of deformation and heat treatment parameters on microstructure evolution of the Ti−25V−15Cr−0.3Si alloy. The aspect (length-to-width) ratio, areas and sizes of the recrystallized grains were measured at different heat treatment temperatures and holding time. The results enable to optimize the processing parameters and control the microstructure under various processing conditions.

2 Experimental

In present investigation, the Ti−25V−15Cr−0.3Si alloy ingot with a diameter of 160 mm was provided by the Northwest Institute for Nonferrous Metal Research, China, and its β transus temperature was calculated to be approximately 454.7 °C using the phase transformation temperature formula in Ref. [15]. The initial microstructure consisted of a single coarse β phase with thin grain boundaries and an average grain size greater than 0.5 mm, as shown in Fig. 1. Cylindrical specimens with 10 mm in diameter and 15 mm in length were machined from the ingot.

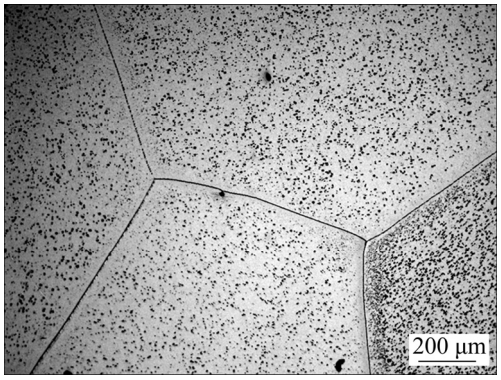

Fig. 1 Microstructure of as-cast Ti−25V−15Cr−0.3Si alloy

To study the SRX behavior of the as-cast Ti−25V−15Cr−0.3Si alloy, isothermal compression tests were performed on a Gleeble 1500 thermal simulator in a deformation temperature range of 950−1050 °C with 50 °C interval, at a strain rate of 0.1 s^{-1} and in a reduction range of 30%−60% with an interval of 15%. Specimens were heated to the required temperature at a rate of 5 °C/s and held at this temperature for 6 min prior to starting isothermal compression experiments to obtain a uniform deformation temperature. The specimens after isothermal compression were submitted to the heat treatment experiments which were performed at 950, 1000 and 1050 °C and the holding time was 5 min, 10 min, 30 min, 1 h, 2 h and 4 h, respectively. After heat treatment, the specimens were quenched in water to preserve the high-temperature microstructure. The quenched specimens were ground, polished and corroded to produce metallographic specimens suitable for observation with an Olympus/PMG3 optical microscope. Details of the experimental process are shown in Fig. 2.

To accurately determine the fractions of SRX, the metallographic image (Fig. 3(a)) should be processed. Firstly, each metallograph was converted into a black-

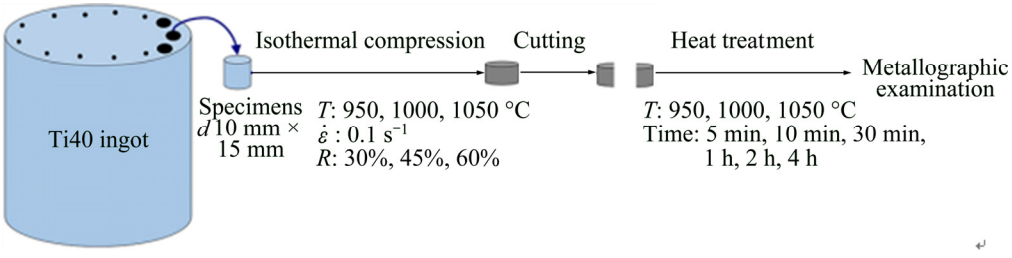

Fig. 2 Details of experimental process

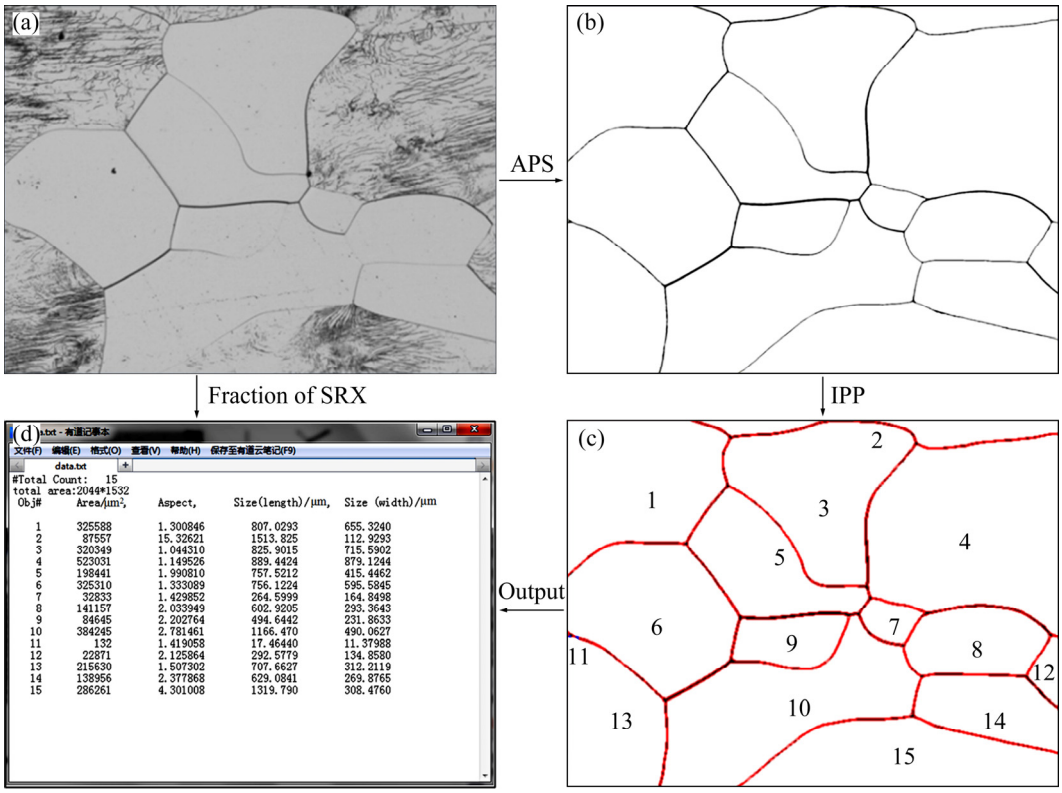

Fig. 3 Image processing procedure (a−c) and grain parameters output (d)

and-white image using image processing software (Adobe Photoshop (APS)) to enhance the grains and grain boundaries, as shown in Fig. 3(b). Secondly, the black-and-white images were imported into a quantitative image analysis software (Image-pro Plus (IPP) 5.0), the scale was set, parameters (such as aspect ratio, area and size) were chosen and each grain was numbered (Fig. 3(c)). Finally, for each grain, parameters such as grain length, width, area and aspect ratio were exported into a text file (Fig. 3(d)). The aspect ratio, area and size of each grain at all of the heat-treatment temperatures and holding time were calculated.

3 Results

3.1 Microstructural evolution after isothermal compression

Figure 4 shows the microstructure evolution of specimens after isothermal compression at height reductions of 30%, 45% and 60% and the deformation temperature of 1000 °C. After plastic deformation, the large β grains were elongated and became flatter, the grain boundaries were widened, and the fine-recrystallization grains were present at grain boundaries. LU et al [16] analyzed the dynamic recrystallization behavior of Ti−25V−15Cr−0.2Si alloy, and found that many dynamic recrystallization grains formed a "necklace" structure along the original grain boundaries. When the height reduction increased from 30% to 60%, the width of the grain boundaries increased from 3−7 μm to 20−53 μm and the number of recrystallized grains increased. However, the degree of recrystallization was low during isothermal compression of the as-cast Ti−25V−15Cr−0.3Si alloy. For example, the recrystallization fraction was determined to be approximately 10% at a height reduction of 60% by the method in Fig. 3. The slow recrystallization during isothermal compression suggested that the deformation energy was stored in the form of distortion energy.

Figure 5 shows the microstructure evolution of specimens after isothermal compression at a height reduction of 60% and deformation temperatures of 950, 1000 and 1050 °C. As the temperature increased, wider and more irregular grain boundaries were formed and finer grains were observed along grain boundaries. The degree of recrystallization did not change significantly with increasing temperature, but the grain size increased, which indicated that the temperature had a more significant effect on the grain size rather than the dynamic recrystallization did.

The microstructures observed in Figs. 4 and 5 indicated that the dynamic recrystallization was minimal and recrystallized grains were small after isothermal compression. Therefore, it is difficult to achieve optimal recrystallization via isothermal compression, which implies that the heat treatment needs to be employed.

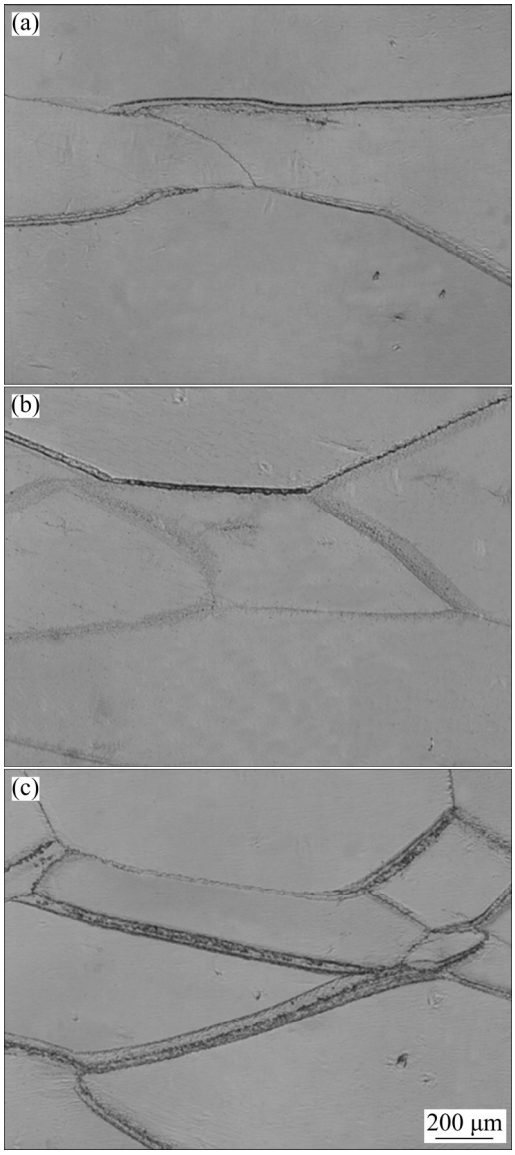

Fig. 4 Microstructural evolution of specimens after isothermal compression at deformation temperature of 1000 °C and different height reductions: (a) 30%; (b) 45%; (c) 60%

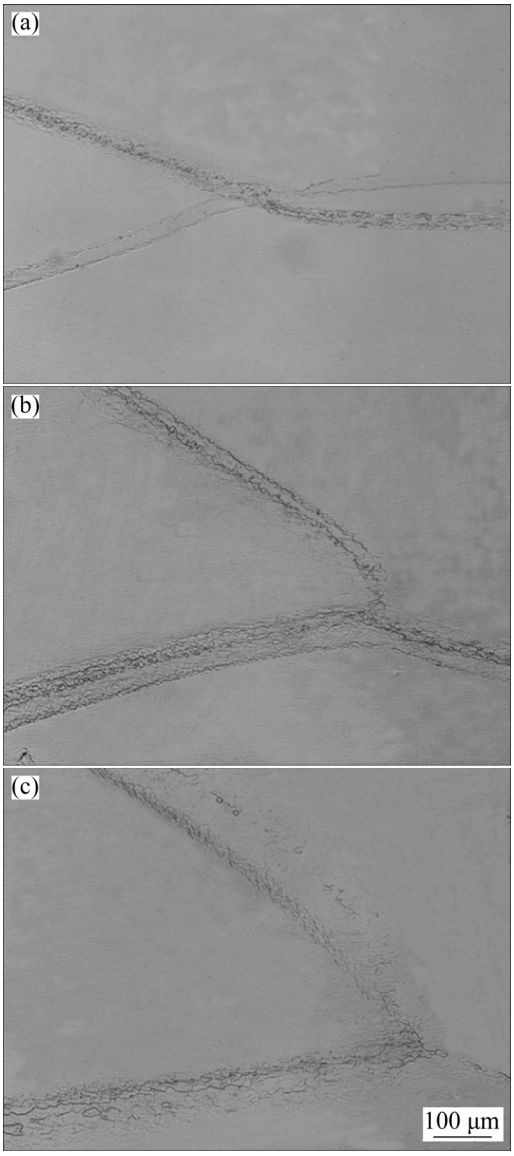

Fig. 5 Microstructural evolution of specimens after isothermal compression at height reduction of 60% and different deformation temperatures: (a) 950 °C; (b) 1000 °C; (c) 1050 °C

3.2 SRX behavior of as-cast Ti−25V−15Cr−0.3Si alloy after annealing at 950 °C

The microstructure of the materials is significantly influenced by the heating temperature and holding time. Investigating microstructural evolution of materials during different heating processes facilitates understanding of the SRX mechanisms [17]. The microstructural evolution of the Ti−25V−15Cr−0.3Si alloy deformed to a height reduction of 30% at 950 °C and then annealed at 950 °C for different time is shown in Fig. 6. The microstructure morphology shows marked changes as the holding time increased. After 10 min, necklace-shaped grains with large aspect ratios precipitated along the grain boundaries (Fig. 6(a)). The aspect ratio of grains decreased and the grain size increased for a holding time of 1 h (Fig. 6(b)). With the holding time from 2 h (Fig. 6(c)) to 4 h (Fig. 6(d)), the number of recrystallized grains decreased and the size of recrystallized grains increased obviously, indicating that the recrystallized grains began to grow with increasing the holding time. And the grain boundaries were smoother than the initial irregular boundaries. Figure 6 demonstrated that both the degree of recrystallization and the size of the recrystallized grains increased as the annealing time increased.

In addition, the secondary phases have been shown to precipitate from the β matrix if the Ti−25V−15Cr−0.3Si alloy is held at high temperatures for a long time [18]. Therefore, it is impossible that the pinning effect of the secondary phases limited dislocation glide and caused dislocation pile-up (Fig. 7), and then a region of high dislocation density, i.e., a high-energy region,

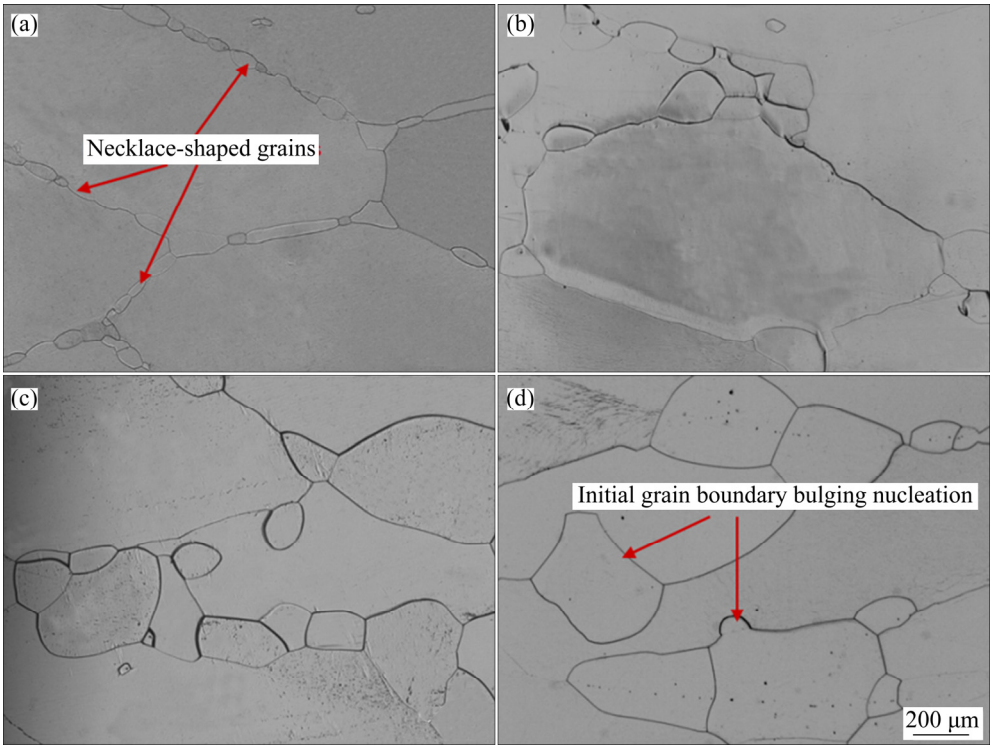

Fig. 6 Microstructural evolution of Ti−25V−15Cr−0.3Si alloy deformed at 950 °C, height reduction of 30% and then annealed at 950 °C for 10 min (a), 1 h (b), 2 h (c) and 4 h (d)

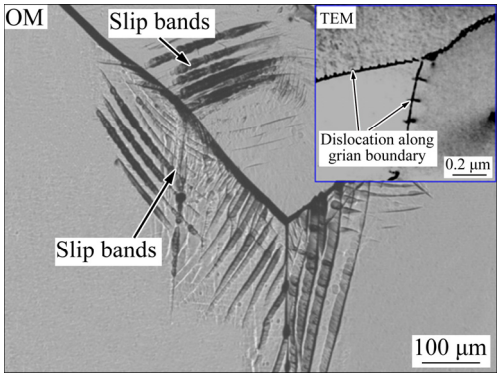

Fig. 7 Slip bands and dislocation pile-up caused by pinning effect of precipitates

was formed, which created an opportunity for dislocation pile-up nucleation. Initial grain boundary bulging nucleation is an example of dislocation pile-up nucleation and can be observed in Fig. 6(d). ZHAO et al [19] also observed a similar phenomenon.

Figure 8 shows the microstructural evolution of specimens deformed to different height reductions and annealed at 950 °C for 1 h. At a height reduction of 30% (Fig 8(a)), the recrystallized grains formed mainly at triple-point grain boundaries. A large number of necklace-shaped recrystallized grains were present along grain boundaries at a height reduction of 45% (Fig. 8(b)) and these newly recrystallized grains at the grain boundaries expanded toward the grain interior by merging with smaller grains at a height reduction of 60% (Fig. 8(c)). Thus, the initial grain boundaries were replaced by new, fine-recrystallized grains and, as the degree of recrystallization increased, the microstructure became more homogeneous.

4 Discussion

4.1 Effects of deformation and heat treatment parameters

Figure 9 shows the effects of height reduction, temperature and heating time on the average aspect ratio, average area and size of the recrystallized grains. With increasing the height reduction, temperature and heating time, the average area and size of the recrystallized grains increased, whereas average aspect ratio of the recrystallized grains decreased. As the height reduction increased from 30% to 60%, the average grain area increased from 2.1×10^4 to 7.4×10^4 μm^2 and the average recrystallized grain size increased from 87−227 to 211−404 μm (Fig. 9(a)). This suggested that the height reduction significantly influenced grain area and grain size because sufficient deformation is the impetus for recrystallization [20]. As annealing time increased (Fig. 9(b)), the size of the recrystallized grains increased from less than 100 μm at 10 min to 200−400 μm at 4 h, i.e., the grain growth was significant as annealing time increased. However, as shown in Fig. 9(c), the grain area did not increase significantly at annealing time between 2 and 4 h, which implied that the annealing time did not

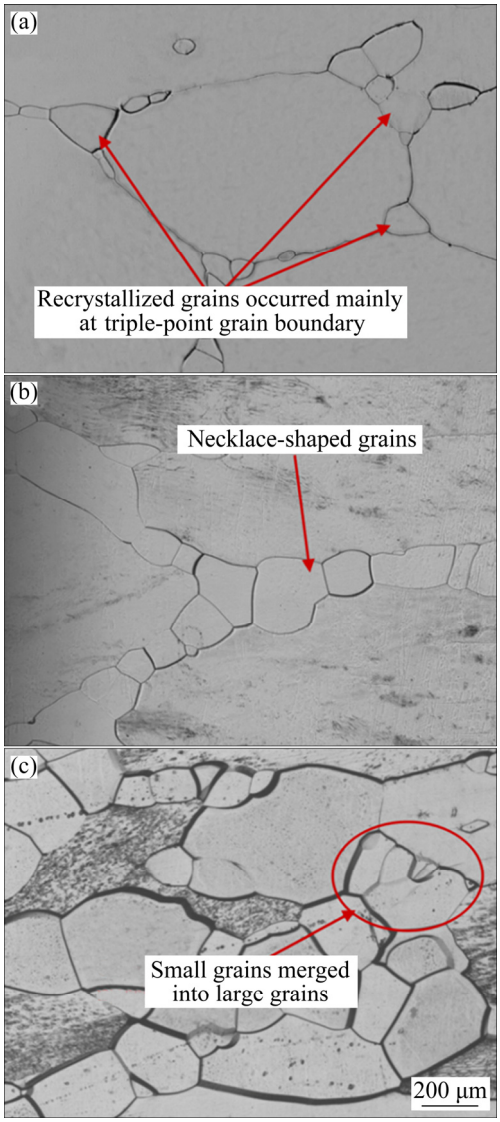

Fig. 8 Microstructural evolution of Ti−25V−15Cr−0.3Si alloy deformed at height reductions of 30% (a), 45% (b), and 60% (c) and then annealed at 950 °C for 1 h

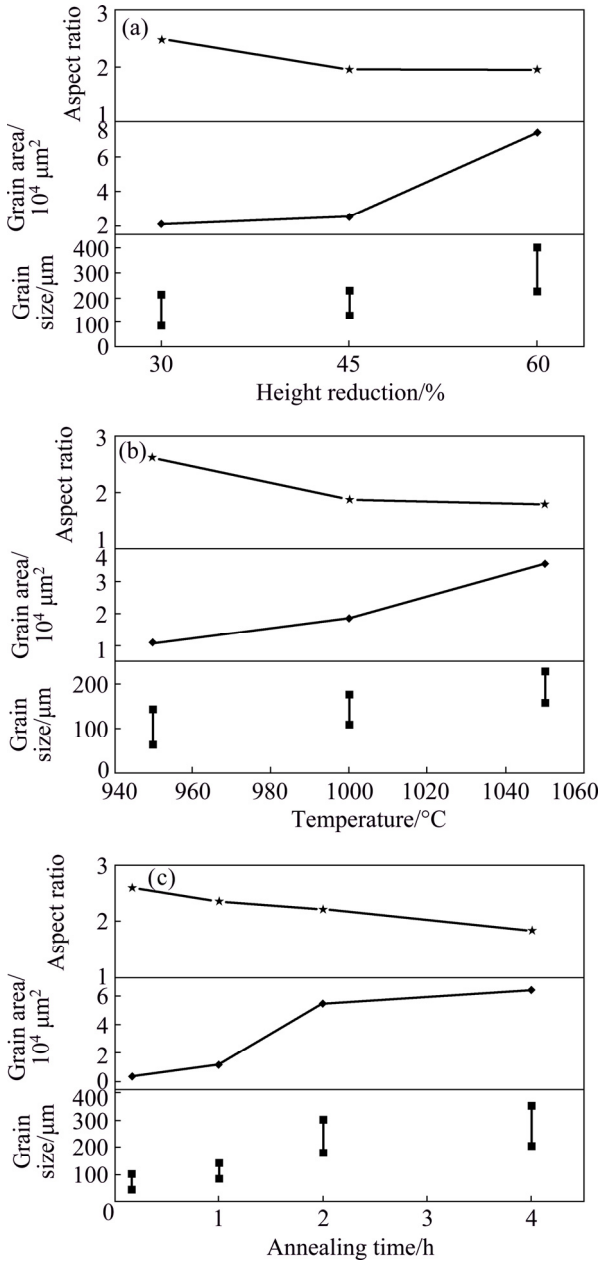

Fig. 9 Effects of height reduction, temperature and heating time on average aspect ratio, area and size of grains for specimens annealed under different conditions: (a) 1000 °C, 1 h; (b) 60%, 0.5 h; (c) 950 °C, 30%

have a significant effect on the grain area when the alloy was deformed to a height reduction of 30% at 950 °C and subsequently annealed at 950 °C for more than 2 h. From Fig. 9, we concluded that the effects of height reduction, temperature and annealing time on aspect ratio of the grains were minimal, while their effects on grain area and grain size were significant. FAN et al [21] investigated the static recrystallization during reheating the TA15 titanium alloy, and pointed out that the microstructure can also be refined by decreasing annealing temperature.

4.2 Precipitation location of secondary phase

By means of the microstructure observation after hot compression (Fig. 5) and previous study [22], it was found that the prior beta grain boundaries were replaced by the new fine dynamically recrystallized grains. Moreover, many dispersion particles were observed and these particles were present in a continuous chain, which is analogous to a grain boundary, as shown in Fig. 10. Furthermore, TEM observation identified the particle with hexagon and sheet morphology, as shown in Fig. 11(a). The electronic diffraction pattern showed that the secondary phase was Ti_5Si_3 phase (Fig. 11(b)), and its crystal structure was hexagonal structure. ANKEM et al [23] researched the silicide formation in Ti−3Al−8V−6Cr−4Zr−4Mo alloy (β-C) and pointed out that the silicide $(Ti, Zr)_5Si_3$ formed in β-C alloy and other similar

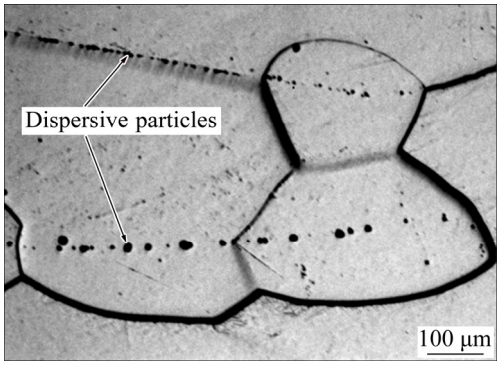

Fig. 10 Dispersive particles observed and present in continuous chain

titanium alloys. FERRERO et al [24] also observed the similar phenomenon in β-C^{TM}. ZHAO et al [18,25] studied the secondary phase extensively in Ti40 alloy after high temperature exposure for a long time, and found that the precipitated dispersion particles were Ti_5Si_3 phase.

To verify the precipitation location of particles, the microstructures of the deformed specimens (950 °C, 45%) and deformed/annealed sample ((950 °C, 45%) + (950 °C, 2 h)) were compared, as shown in Fig. 12. It is easy to find out that the black dispersion particles in continuous chain precipitated along the prior β grain boundaries. Moreover, the precipitates were coarsened

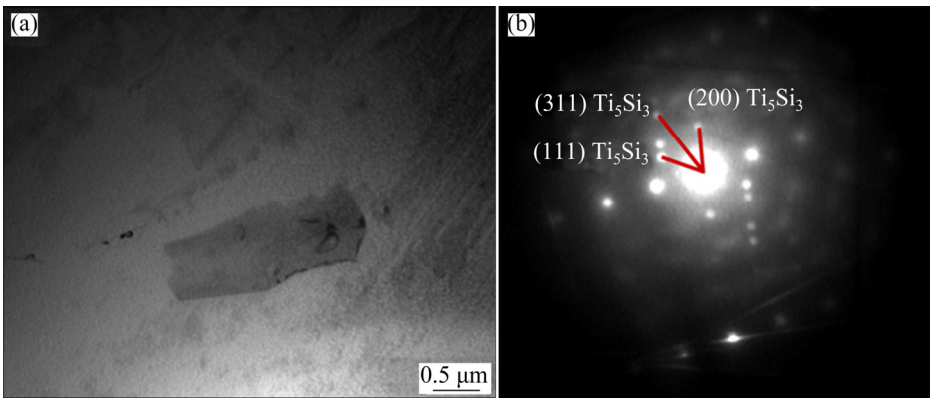

Fig. 11 TEM micrographs of silicide in Ti−25V−15Cr−0.3Si alloy heat-treated at 1000 °C for 10 h: (a) TEM bright field image; (b) SAD pattern and indexing

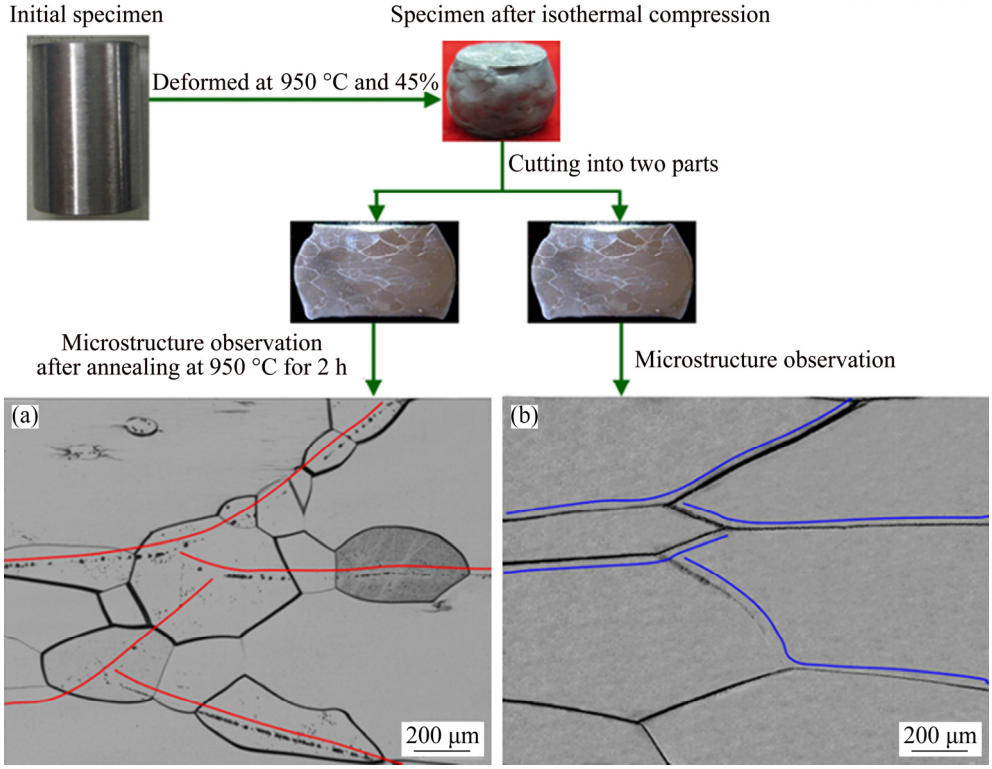

Fig. 12 Procedure used to determine precipitation location of secondary phase by comparing microstructures between sample deformed at 950 °C and 45% (a) and sample deformed at 950 °C and 45% following by heat treatment at 950 °C for 2 h (b)

and the size of precipitates increased with increasing the heat treatment time, as shown in Fig. 13. It can be seen from Fig. 13 that the quantity of precipitate particles also increased with the increase of heating time. WU et al [26] analyzed the amount and distribution of the precipitates for a weathering steel microalloyed with vanadium and pointed out that the precipitates distributed over the grain boundaries, sub-grain boundaries, dislocation lines, deformation bands and other crystal defects.

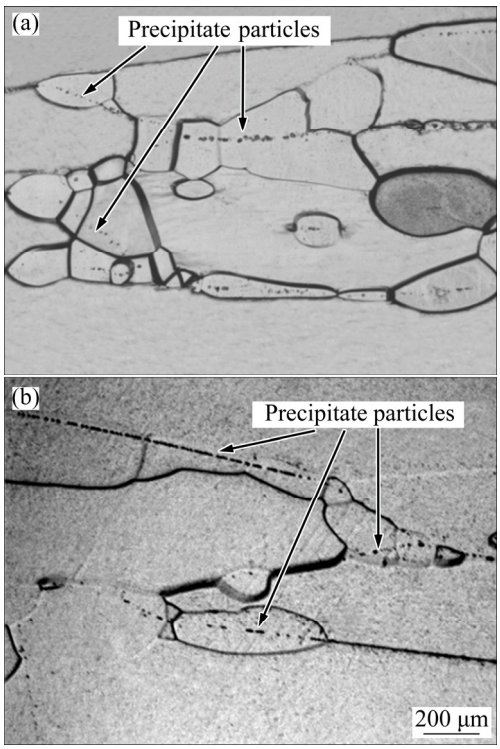

Fig. 13 Dispersive particles precipitated at 950 °C for different heating time: (a) 1 h; (b) 10 h

5 Conclusions

1) Dynamic recrystallization was minimal and the recrystallized grains were small during isothermal compression of the as-cast Ti−25V−15Cr−0.3Si alloy; the deformation energy was stored in the form of distortion energy.

2) Under the deformation condition of 950 °C and 30% height reduction, grain growth was high as the annealing time increased from 10 min to 2 h; grain growth was minimal for annealing time between 2 and 4 h. Larger grain area and size as well as a more homogeneous microstructure were obtained when the height reduction increased from 30% to 60%.

3) The effects of height reduction, temperature and annealing time on the aspect ratio of the grains were minimal; the height reduction had a significant effect on grain area and grain size, while the effects of annealing time and temperature were minimal.

4) Many dispersion particles were observed to form a continuous chain; the particles which precipitated along the initial grain boundaries were identified to be Ti_5Si_3 phase.

References

[1] ZHAO Yong-qing, ZHAO Xiang-miao, ZHU Kang-ying, LUO Guo-zhen, ZHOU Lian. Burn resistant titanium alloy [J]. Rare Metal Materials and Engineering, 1996, 25: 1−6. (in Chinese)

[2] IVASISHIN O M, MARKOVSKY P E, MATVIYCHUK Y V, SEMIATIN S L. Precipitation and recrystallization behavior of beta titanium alloys during continuous heat treatment [J]. Metallurgical and Materials Transactions A, 2003, 34: 147−158.

[3] SEMIATIN S L, SUKONNIK I M, SEETHARAMAN V. An analysis of static recrystallization during continuous, rapid heat treatment [J]. Metallurgical and Materials Transactions A, 1996, 27: 2051−2053.

[4] SEMIATIN S L, KNISLEY S L, FAGIN P N, ZHANG F, BARKER D R. Microstructure evolution during alpha-beta heat treatment of Ti−6Al−4V [J]. Metallurgical and Materials Transactions A, 2003, 34: 2377−2386.

[5] SEMIATIN S L, BROWN T M, GOFF T A, FAGIN P N, BARKER D R, TURNER R E, MURRY J M, MILLER J D, ZHANG F. Diffusion coefficients for modeling the heat treatment of Ti−6Al−4V [J]. Metallurgical and Materials Transactions A, 2004, 35: 3015−3018.

[6] SEMIATIN S L, STEFANSSON N, DOHERTY R D. Prediction of the kinetics of static globularization of Ti−6Al−4V [J]. Metallurgical and Materials Transactions A, 2005, 36: 1372−1376.

[7] STEFANSSON N, SEMIATIN S L, EYLON D. The kinetics of static globularization of Ti−6Al−4V [J]. Metallurgical and Materials Transactions A, 2002, 33: 3527−3534.

[8] STEFANSSON N, SEMIATIN S L. Mechanisms of globularization of Ti−6Al−4V during static heat treatment [J]. Metallurgical and Materials Transactions A, 2003, 34: 691−698.

[9] ZHEREBTSOV S, MURZINOVA M, SALISHCHEV G, SEMIATIN S L. Spheroidization of the lamellar microstructure in Ti−6Al−4V alloy during warm deformation and annealing [J]. Acta Materialia, 2011, 59: 4138−4150.

[10] XU Xin, DONG Li-min, BA Hong-bo, ZHANG Zhi-qiang, YANG Rui. Hot deformation behavior and microstructural evolution of beta C titanium alloy in β phase field [J]. Transactions of Nonferrous Metals Society of China, 2016, 26: 2874−2882.

[11] LI Hui-min, LI Miao-quan, LUO Jiao, WANG Ke. Microstructure and mechanical properties of heat-treated Ti−5Al−2Sn−2Zr−4Mo−4Cr [J]. Transactions of Nonferrous Metals Society of China, 2015, 25: 2893−2900.

[12] FANG Hong-ze, CHEN Rui-run, ANTON G, GUO Jing-jie, DING Hong-sheng, SU Yan-qing, FU Heng-zhi. Effect of cyclic heat treatment on microstructures and mechanical properties of directionally solidified Ti−46Al−6Nb alloy [J]. Transactions of Nonferrous Metals Society of China, 2015, 25: 1872−1880.

[13] SONG Lin, PENG Cong, XU Xiang-jun, YOU Li, WANG Yan-li, LIN Jun-pin. ω_o phase precipitation in annealed high Nb containing TiAl alloys [J]. Progress in Natural Science−Materials International, 2015, 25: 147−152.

[14] FURUHARA T, MAKI T, MAKIN T. Microstructure control by thermomechanical processing in β-Ti-15-3 alloy [J]. Journal of Materials Processing Technology, 2001, 117: 318−323.

[15] Editing Team of Rare Metal Materials Processing Handbook. Rare metal materials processing handbook [M]. Beijing: Metallurgical

Industry Press, 1984. (in Chinese)
[16] LU Shi-qiang, OUYANG De-lai, CUI Xia, WANG Ke-lu. Dynamic recrystallization behavior of burn resistant titanium alloy Ti−25V−15Cr−0.2Si [J]. Transactions of Nonferrous Metals Society of China, 2016, 26: 1003−1010.
[17] XUE Chen, ZENG Wei-dong, XU Bin, LIANG Xiao-bo, ZHANG Jian-wei, LI Shi-qiong. B_2 grain growth and particle pinning effect of Ti−22Al−25Nb orthorhombic intermetallic alloy during heating process [J]. Intermetallics, 2012, 29: 41−47.
[18] ZHAO Yong-qing, QU Heng-lei, ZHU Kang-ying, WU Huan, LIU Chun-li, ZHOU Lian. The second phases in Ti40 burn resistant alloy after high temperature exposure for a long time [J]. Journal of Alloys and Compounds, 2002, 333: 165−169.
[19] ZHAO Yong-qing, SHU Ying, ZENG Wei-dong, WU Wei-lu, WU Huan, ZHOU Yi-gang, YANG Hai-ying, LI Qian. Dynamic recrystallization behavior of highly stabilized β Ti40 titanium alloy [J]. Rare Metal Materials and Engineering, 2009, 38: 1432−1436. (in Chinese)
[20] WANG Kai-xuan, ZENG Wei-dong, ZHAO Yong-qing, LAI Yun-jin, ZHANG Xue-min, ZHOU Yi-gang. Flow behaviour and microstructural evolution of Ti-17 alloy with lamellar microstructure during hot deformation in β phase field [J]. Materials Science & Technology, 2010, 27: 21−28.
[21] FAN X G, YANG H, GAO P F, ZUO R, LEI P H. The role of dynamic and post dynamic recrystallization on microstructure refinement in primary working of a coarse grained two-phase titanium alloy [J]. Journal of Materials Processing Technology, 2016, 234: 290−299.
[22] ZHU Yan-chun, ZENG Wei-dong, ZHAO Yong-qing, SHU Ying, ZHANG Xue-min. Effect of processing parameters on hot deformation behavior and microstructural evolution during hot compression of Ti40 titanium alloy [J]. Materials Science and Engineering A, 2012, 552: 384−391.
[23] ANKEM S, BANERJEE D, MCNEISH D J, WILLIAMS J C, SEAGLE S R. Silicide formation in Ti−3Al−8V−6Cr−4Zr−4Mo [J]. Metallurgical Transactions A, 1987, 18: 2015−2025.
[24] FERRERO J G, WOOD J R, RUSSO P A. Beta titanium alloy in the 1990's [M]. Warrendale: TMS, 1993.
[25] ZHAO Yong-qing, QU Heng-lei, ZHU Kang-ying, WU Huan, LIU Cai-li, ZHOU Lian. The second phases in a burn resistant alloy-Ti40 [J]. Rare Metal Materials and Engineering, 2001, 30: 413−417. (in Chinese)
[26] WU H Y, DU L X, AI Z R, LIU X H. Static recrystallization and precipitation behavior of a weathering steel microalloyed with vanadium [J]. Journal of Materials Science & Technology, 2013, 29: 1197−1203.

铸态 Ti−25V−15Cr−0.3Si 钛合金静态再结晶过程中的二次相析出位置及显微组织演变

朱艳春[1]，黄庆学[1,2]，石晓辉[2]，帅美荣[1]，曾卫东[3]，赵永庆[4]，黄志权[1]，马立峰[1]

1. 太原科技大学 太原重型机械装备协同创新中心，太原 030024；
2. 太原理工大学 材料科学与工程学院，太原 030024；
3. 西北工业大学 凝固技术国家重点实验室，西安 710072；
4. 西北有色金属研究院，西安 710016

摘 要：利用热压缩和热处理实验研究铸态 Ti−25V−15Cr−0.3Si 钛合金的显微组织演变和二次相析出位置。研究在不同热处理温度和时间下晶粒的平均长宽比、平均面积和尺寸，分析变形量和退火参数对晶粒面积和尺寸的影响。结果表明，晶粒尺寸受变形量和退火时间影响显著，在 950 °C、变形量为 30%、当退火时间从 10 min 增加至 2 h 时，晶粒明显长大；而当退火时间为 2~4 h 时，晶粒长大缓慢。此外，还观察到大量弥散质点以连续的链状存在，显微组织观察和 TEM 衍射花样分析证实沿着原始晶界析出的弥散质点为 Ti_5Si_3 相。

关键词：Ti−25V−15Cr−0.3Si 钛合金；静态再结晶；显微组织演变；晶粒尺寸；二次相；析出位置

(Edited by Wei-ping CHEN)